Chem

Convergent synthesis and protein binding of vicinal difluorides by stereodivergent C–C bond formation

Graphical abstract

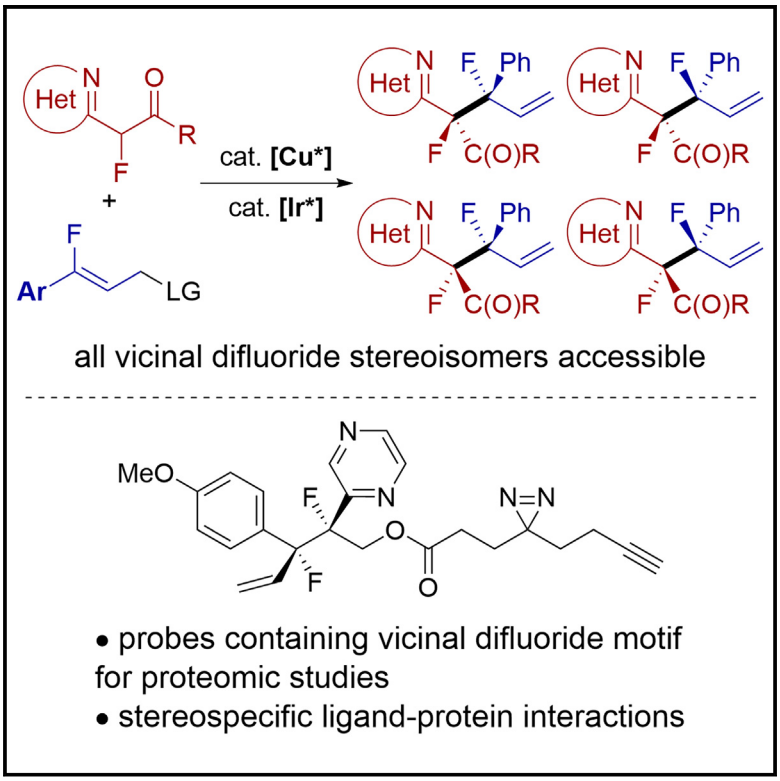

Highlights

- Catalyst-controlled synthesis of all four stereoisomers of vicinal difluorides
- Experiments and computations confirm the *gauche* relationship between two fluorides
- Development of probes containing the vicinal difluoride motif for proteomic studies
- Configuration and conformation of vicinal difluorides affect protein binding

Authors

Yehao Qiu, Vienna C.J.X. Thomas, Tommaso Fantoni, ..., Trevor W. Butcher, Daniel K. Nomura, John F. Hartwig

Correspondence

dnomura@berkeley.edu (D.K.N.), jhartwig@berkeley.edu (J.F.H.)

In brief

Vicinal difluorides control the conformation about C–C single bonds by electronic effects and can be valuable substructures of biologically active compounds. However, their stereoselective synthesis has been cumbersome. Here, we report the synthesis of all four stereoisomers of vicinal difluorides by C–C bond formation with catalyst-controlled stereoselectivity. Probes containing the vicinal difluoride subunit were developed, and chemoproteomic studies suggest that absolute configuration and relative conformation of the two fluorides significantly affect protein binding.

Qiu et al., 2024, Chem *10*, 3709–3721
December 12, 2024
https://doi.org/10.1016/j.chempr.2024.08.024

CellPress

Chem

CellPress

Article

Convergent synthesis and protein binding of vicinal difluorides by stereodivergent C–C bond formation

Yehao Qiu,[1,2] Vienna C.J.X. Thomas,[1,2] Tommaso Fantoni,[1] Reichi Chen,[1] Xingyu Jiang,[1] Zhi-Tao He,[1] Trevor W. Butcher,[1] Daniel K. Nomura,[1,*] and John F. Hartwig[1,3,*]

[1]Department of Chemistry, University of California, Berkeley, CA 94720, USA

[2]These authors contributed equally

[3]Lead contact

*Correspondence: dnomura@berkeley.edu (D.K.N.), jhartwig@berkeley.edu (J.F.H.)

https://doi.org/10.1016/j.chempr.2024.08.024

THE BIGGER PICTURE Configurations and conformations of organic molecules affect properties and function. The conformation about acyclic C–C single bonds is difficult to control, leading to guidelines that limit such units in drug molecules. Vicinal difluorides contain one fluorine on two contiguous saturated carbons and adopt specific conformations, but stereoselective synthesis of such difluorides is difficult. We report a catalytic method to synthesize all four stereoisomers of vicinal difluorides by forming the C–C bond between two mono-fluorinated units with high yield, stereoselectivity, and tolerance of heteroaryl groups that are common in drug molecules. Chemical probes containing the vicinal difluoride motif were developed, and proteomic studies provide evidence for stereospecific ligand-protein interactions by the vicinal difluorides. This strategy will be valuable for controlling the conformation of highly substituted C–C bonds and enabling the design of new classes of biologically active molecules.

SUMMARY

Vicinal difluorides adopt defined conformations due to the electronic properties of fluorine. Therefore, they could be valuable for controlling the constellation of functional groups about acyclic C–C bonds in organic molecules if all stereoisomers of the difluorides could be synthesized. However, stereoselective synthesis of vicinal difluorides has been cumbersome. The location of functional groups within organic molecules is important because it influences function, particularly biological function. We report a catalytic synthesis of acyclic vicinal difluoride stereoisomers by C–C bond formation between two monofluoro units, along with crystallographic and computational data showing that the *gauche* relationship of two fluorides causes substituents to occupy defined positions about the C(sp^3)–C(sp^3) bond. Photoreactive chemical probes tethered to vicinal difluorides showed that difluorides bind more strongly than the analogous monofluorides, which possess less defined conformations, and that individual stereoisomers of the difluorides bind distinctly to the human proteome.

INTRODUCTION

The absolute and relative configuration of stereogenic centers and the conformations around rotatable bonds define the structure of organic molecules and resulting properties, such as the ability to bind to proteins, nucleic acids, and carbohydrates.[1–5] Many strategies have been developed to control the conformations of molecules that contain planar functional groups, such as amides or alkenes,[1,6–9] saturated rings,[10–18] or two arenes connected by a single bond.[19–23] However, strategies to control the conformation about acyclic bonds connecting two sp^3-hybridized carbon atoms are more limited because the barrier to rotation around a C(sp^3)–C(sp^3) bond is usually low[24] and because conformers resulting from rotation around a C(sp^3)–C(sp^3) bond are often similar in energy.[25,26] Indeed, guidelines for designing molecules for medicinal chemistry recommend limiting the number of rotatable bonds in a molecule.[27,28]

Vicinal difluoride units are defined as two adjacent carbon atoms bonded to one fluorine atom each, most commonly referring specifically to a unit containing two saturated carbons connected to one fluorine each.[29] The size of a fluorine atom is similar to that of a hydrogen atom,[30] so a vicinal difluoride motif

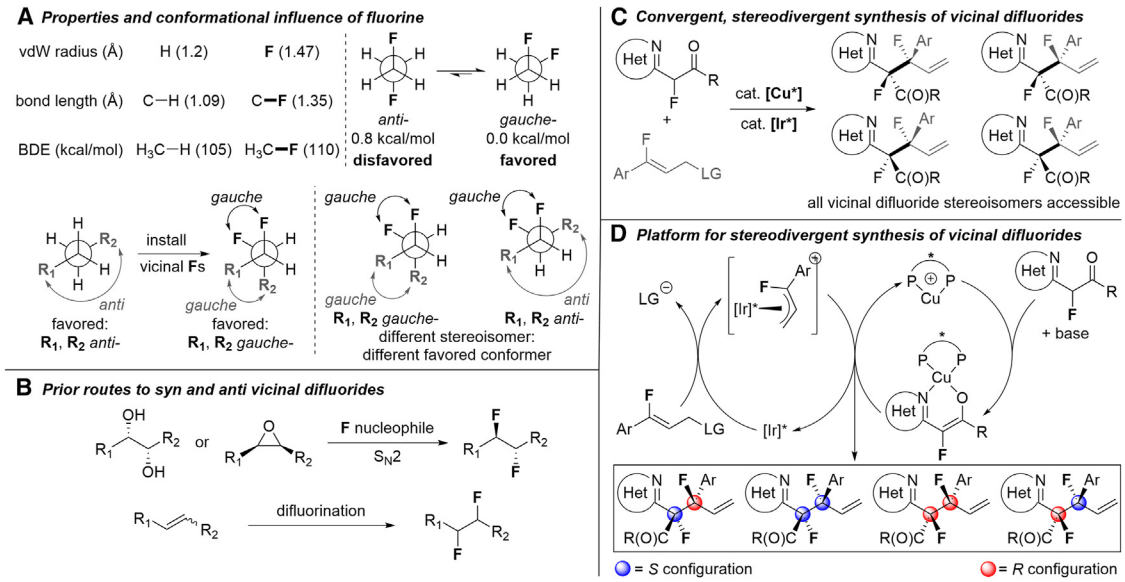

Figure 1. Stereodivergent synthesis of vicinal difluorides as a novel strategy to control the confirmation of acyclic C(sp^3)–C(sp^3) bonds

(A) Structural features of vicinal difluorides.

(B) Prior syntheses of vicinal difluorides by stereospecific or non-stereoselective C–F bond formations.

(C) This work: modular synthesis of vicinal difluorides by stereodivergent C–C bond formation.

(D) Reaction design and the proposed catalytic cycle.

containing two sp^3-hybridized carbon atoms is sterically similar to that of two adjacent methine units. In addition, most C(sp^3)–F bonds are stable (bond dissociation energy > 110 kcal/mol, Figure 1A, top left),[31] making the "C–F" bond resistant to most chemical transformations. As a result, replacement of a C(H)–C(H) unit, in which both carbons are sp^3-hybridized, by an analogous saturated vicinal difluoride C(F)–C(F) unit does not significantly change the steric properties or the chemical reactivity of the compound.

Yet, saturated vicinal difluorides often adopt a defined conformation about the C(sp^3)–C(sp^3) bond.[29,32,33] The stabilizing hyperconjugation between the σ^* orbital of the C–F bond and an adjacent, occupied σ orbital causes a saturated vicinal difluoride motif to favor the conformer in which the two F atoms are positioned *gauche* to each other (shown for difluoroethane at the right of Figure 1A).[34–37] This stable *gauche* relationship between two adjacent fluorine atoms allows one to predict the relative position (e.g., *gauche* or *anti*) of the other substituents (Figure 1A, bottom left) in the most favorable conformation. Because the most favorable conformer of each stereoisomer of a given vicinal difluoride compound is different, one can control the relative position of substituents about the C–C bond by synthesizing the corresponding stereoisomer (Figure 1A, bottom right). Indeed, the active conformation of γ-aminobutyric acid (GABA) bound to GABA receptors was deduced from the stable gauche conformation of vicinal fluoride analogs of GABA, which were prepared as individual stereoisomers in 12 steps.[38]

Although vicinal difluorides are potentially valuable substructures, the construction of such subunits has been limited or cumbersome, or both, particularly with control of absolute and relative configuration. Current syntheses of saturated vicinal difluorides have followed two strategies, both involving the formation of C–F bonds with the connecting C–C bond in place (Figure 1B): (1) two sequential nucleophilic substitution reactions between fluoride nucleophiles and an epoxide or a diol,[39–41] and (2) the difluorination of alkenes.[42–48] The route involving nucleophilic substitution often requires harsh, toxic reagents, such as HF or SF_4,[40,41] that cannot be used in a typical laboratory and are limited in their tolerance of functional groups even when used in a specialized facility, and the synthesis of a series of stereoisomers is challenging[49] because the substitution reactions are stereospecific. The second approach involving enantioselective difluorination of alkenes is limited in scope and requires single olefin stereoisomers to occur with high diastereoselectivity.[50–52]

We envisioned that these synthetic challenges could be addressed and the effect of two adjacent fluorine atoms on conformation and consequent protein binding could be evaluated by an alternative, convergent strategy that forms the C–C bond within the vicinal difluoride unit and proteomic analysis of the resulting structures. No method is known to form the C–C bond between two saturated carbons in vicinal difluorides by joining two different fluorine-containing units, let alone a method that occurs enantioselectively or one that controls the configurations of the two stereogenic centers individually. However, if such a reaction that controls absolute and relative configuration could be realized, then the impact of fluorine atoms at two vicinal carbons could be assessed by comparing the binding of the individual stereoisomers to a proteome and comparing the binding of these compounds to that of analogs containing a single fluorine atom.

To achieve such bond formation, we devised a strategy involving allylic substitution. Catalytic allylic substitution could form the carbon–carbon bond, and methods that combine one

transition-metal catalyst to control the configuration of the nucleophile[53,54] and another to control the configuration of the electrophile[55–57] could, thereby, dictate the absolute and relative configurations of the two stereogenic centers. We invoked allylic substitutions because the scope of reactions of allyliridium catalysts that we have studied encompasses those with a fluorine atom in one of the two coupling partners.[54,55] At the same time, we recognized that application of this strategy to form vicinal difluorides would confront several challenges when joining two fluorine-containing units, particularly with stereochemical control. Fluorine is the most electronegative element, but, paradoxically, a fluorine atom makes the carbon to which it is attached less electrophilic.[58–63] Thus, it was unclear if a fluorinated allylic electrophile would react with a fluorinated nucleophile to form the central C–C bond. Moreover, the repulsion between two approaching C–F units is stronger than that between one C–F and one "C–H" unit due to the high electron density around fluorine atoms, making it uncertain whether two fluorinated partners would react to form the C–C bond and whether the electronic properties would allow all stereoisomers to be formed with selectivity dictated by the catalyst rather than the reactants. Finally, the presence of multiple substituents around the vicinal carbons accompanying the fluorine atoms made it unclear whether the two small fluorine atoms would dictate the conformation about the newly formed C–C bond in the product or whether the conformation would be controlled by the steric or electronic properties of the other groups.

Despite these challenges, we show that the convergent construction of all four stereoisomers of a vicinal difluoride motif occurs stereoselectively by forming the C(sp^3)–C(sp^3) bond between two achiral or racemic mono-fluorinated building blocks in a single reaction catalyzed by copper and iridium complexes and that the presence and stereochemical disposition of the fluorine atoms strongly influences protein binding. The appropriate electrophilicity was achieved by adjusting the leaving group, and selective binding of single isomers to specific proteins controlled by the vicinal difluoride unit was revealed by attaching a photoreactive chemical probe to the vicinal difluorides and their monofluoride analogs and analyzing binding to the proteome of human embryonic kidney (HEK293T) cells. Distinct binding of one of the four stereoisomers to the thioredoxin reductase TXNRD2 was identified and confirmed, showing how stereodivergent synthetic strategies[64] can enhance selective binding of molecules with acyclic core structures.

RESULTS AND DISCUSSION

Formation of vicinal difluorides

To achieve a convergent synthesis of vicinal difluorides by formation of the C–C bond using the coupling of a fluoroallyl electrophile and an α-fluorinated pronucleophile, we followed our strategy involving a combination of copper and iridium catalysts and azaarene-substituted enolate nucleophiles.[53,54] In this reaction design, a Lewis-acidic copper catalyst, which is ligated by a chiral bisphosphine, would coordinate to the nitrogen and the oxygen atom of a 2-fluoro-2-azaarylcarbonyl compound as pronucleophile and generate the corresponding chiral Cu-enolate intermediate in the presence of a base. This Cu-enolate would react with a chiral, cationic (3-fluoroallyl)iridium species to generate the vicinal difluoride product (Figures 1C and 1D). After thorough investigations of the effect of the bisphosphine ligand bound to copper on the yield and stereoselectivity of the catalytic allylic substitution between methyl 2-fluoro-2-(pyridin-2-yl)acetate (**1a**) and (*Z*)-3-fluoro-3-phenylallyl methyl carbonate (**2aα**) with (R_a,*R*,*R*)-[**Ir**] as the iridium cocatalyst (see Tables 1 and S1), we found that reactions with the ligand (*R*,*R*)-Ph-BPE (**L6**) or its enantiomer (*ent*-**L6**) afforded the desired vicinal difluoride product **3a** or **5a** in 83% or 80% yield, respectively, with excellent stereoselectivity (15:1 diastereomeric ratio [dr], 99% ee for **3a** and 20:1 dr, 97% ee for **5a**; Table 1, entries 8, 9). The reaction in the presence of a WALPHOS-type ligand **L2** and (R_a,*R*,*R*)-[**Ir**] formed product **5a** in high yield and with high stereoselectivity (Table 1, entry 2), but the reaction with the enantiomer of **L2** (*ent*-**L2**) afforded product **3a** with low stereoselectivity. (Table 1, entry 3). This mismatch of selectivity with ligand **L2** was not observed in allylic substitutions between two non-fluorinated building blocks under similar reaction conditions[53] and is consistent with our previous discussion that repulsion between two approaching fluorine atoms makes the control of stereochemistry difficult. Several pronucleophiles containing five-membered heterocyclic arenes reacted with **2aα** and formed the corresponding vicinal difluorides in low yields (Table 1, entry 12) but were known to react with cinnamyl methyl carbonate, which is the non-fluorinated analog of **2aα**, to afford the corresponding mono-fluorinated products in high yields under similar reaction conditions.[54] The contrast between these outcomes is consistent with the aforementioned challenge that a fluorine atom makes the carbon to which it is attached less electrophilic. To increase the electrophilicity of the fluoroallyl unit and improve the yield of the reaction, we tested the electrophile **2aβ** (Figure 2A, condition B) that contains a more reactive leaving group, −OTroc (Troc = 2,2,2-trichloroethoxycarbonyl), than that in a methyl carbonate. Indeed, we found that reactions of **2aβ** with fluorinated pronucleophiles containing five-membered heteroarenes generally formed vicinal difluorides in higher yields than those with **2aα** (Table 1, entries 13, 14). Control experiments indicated that both the Cu/bisphosphine catalyst and the Ir catalyst were necessary for this reaction (Table 1, entries 10, 11).

Examples of pronucleophiles that underwent this catalytic reaction are shown in Figure 2A. A series of α-fluoroacetates and α-fluoroketones that contained six-membered heteroarenes, such as pyridines, pyrazines, pyrimidines, and quinolines, reacted with the fluorinated electrophiles **2aα** or **2aβ** to form the corresponding vicinal difluoride products **3a**, **3c**–**3g**, **3i**, and **3n** in good yields (69%–96%), with acceptable to high diastereoselectivity (dr 5:1–20:1) and excellent enantioselectivity (ee 97%–99%). α-Fluoroacetates containing five-membered heteroarenes, such as benzoxazole, benzothiazole, and benzimidazole, also underwent the catalytic reaction to afford products **3b**, **3m**, and **3h** in 83%–85% yield, with 8:1–12:1 dr, and >99% enantiomeric excess. In addition to α-fluoro-α-azaaryl acetates and ketones, α-fluoro-acetamides containing the benzoxazole and the benzothiazole moieties underwent allylic substitution to form products **3l** and **3j** in good yields (78% for **3j**, 99% for **3l**) and with high stereoselectivity (dr 9:1, ee 98% for **3j**; dr 14:1, ee 95% for **3l**). Heteroaryl groups that contain three or

Table 1. Development of reaction conditions for the allylic substitution between 2-fluoro-2-azaarylacetates 1a, 1b, and (*Z*)-3-fluoro-3-phenylallylic electrophile 2aα or 2aβ

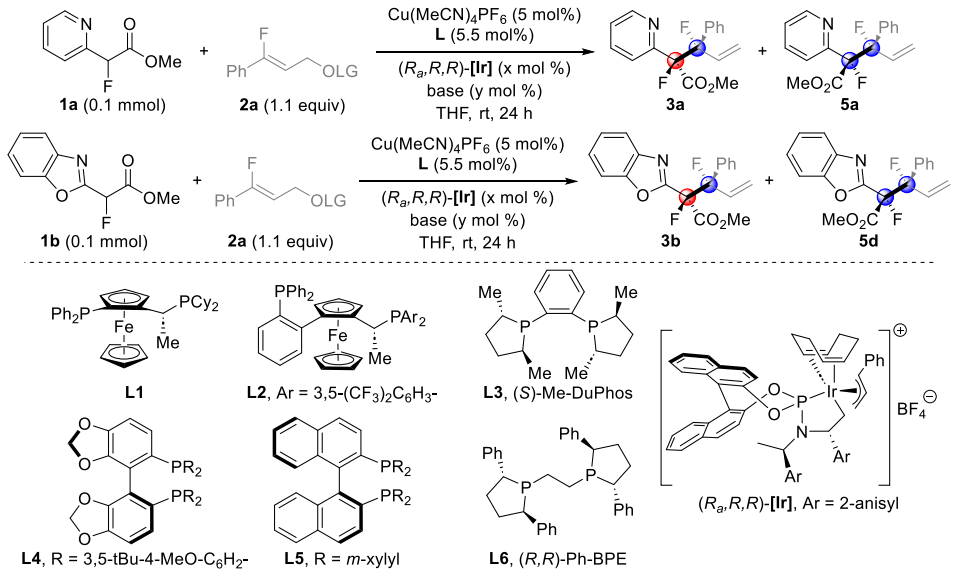

Entry	Nu	–OLG	Ligand	x	Base	y	Yield (%)[a]	dr[b]	ee (%)[c]
1	**1a**	$-OCO_2Me$	**L1**	5	K_2CO_3	120	90	1:2	*n.d.*
2	**1a**	$-OCO_2Me$	**L2**	5	K_2CO_3	120	88	1:12	>99
3	**1a**	$-OCO_2Me$	*ent*-**L2**	5	K_2CO_3	120	85	3:1	*n.d.*
4	**1a**	$-OCO_2Me$	**L3**	5	K_2CO_3	120	16	1:1	*n.d.*
5	**1a**	$-OCO_2Me$	**L4**	5	K_2CO_3	120	53	2:1	*n.d.*
6	**1a**	$-OCO_2Me$	**L5**	5	K_2CO_3	120	88	1:4	*n.d.*
7	**1a**	$-OCO_2Me$	**L6**	5	K_2CO_3	120	77[d]	13:1	>99
8	**1a**	$-OCO_2Me$	**L6**	5	K_2CO_3	50	83[d]	15:1	99
9	**1a**	$-OCO_2Me$	*ent*-**L6**	5	K_2CO_3	50	80[d]	1:20	97
10	**1a**	$-OCO_2Me$	**L6**	0	K_2CO_3	50	0	N/A	N/A
11	**1a**	$-OCO_2Me$	none[e]	5	K_2CO_3	50	0	N/A	N/A
12	**1b**	$-OCO_2Me$	**L6**	3	K_2CO_3	100	43	3:1	*n.d.*
13	**1b**	–OTroc	**L6**	3	K_2CO_3	100	83[d]	12:1	>99
14	**1b**	–OTroc	*ent*-**L6**	3	K_2CO_3	100	73[d]	1:5	>99

[a]Combined NMR yield of both diastereomers, unless specified otherwise.
[b]The ratio of **3a** to **5a** or **3b** to **5d**.
[c]*n.d.* stands for not determined.
[d]Isolated yield of one diastereomer.
[e]In the absence of $Cu(MeCN)_4PF_6$ and ligand.

four nitrogen atoms, such as a triazine (**3o**) and a tetrazole (**3k**), were also compatible with this reaction. The moderate diastereoselectivity (dr 3:1) for the formation of compound **3o**, presumably, results from weak binding of the nitrogen atom in the triazine to the Lewis-acidic copper, due to steric effects.

Figure 2B shows a series of (*Z*)-3-fluoro-3-arylallyl methyl carbonates containing substituted aryl or heteroaryl groups that underwent the catalytic allylic substitution with α-fluoroacetate **1g** and formed the corresponding vicinal difluorides in good yields (57%–85%) and with high stereoselectivity (dr 8:1–24:1, ee 98%–99%). Reactions of (*Z*)-3-fluoro-3-arylallyl methyl carbonates containing electron-rich, electron-neutral, and electron-poor aryl groups (**4a**–**4g**) afforded the products in good yield and with excellent diastereo- and enantioselectivity. This catalytic method tolerated structures with versatile synthetic handles, such as mono- or di-halogenated aryl rings (**4a**, **4b**, **4f**), Boc-protected aniline (**4k**), and a carbonate-masked benzylic alcohol (**4j**). Simple heteroarenes, such as furan (**4h**) and thiophene (**4i**), also were compatible with this transformation.

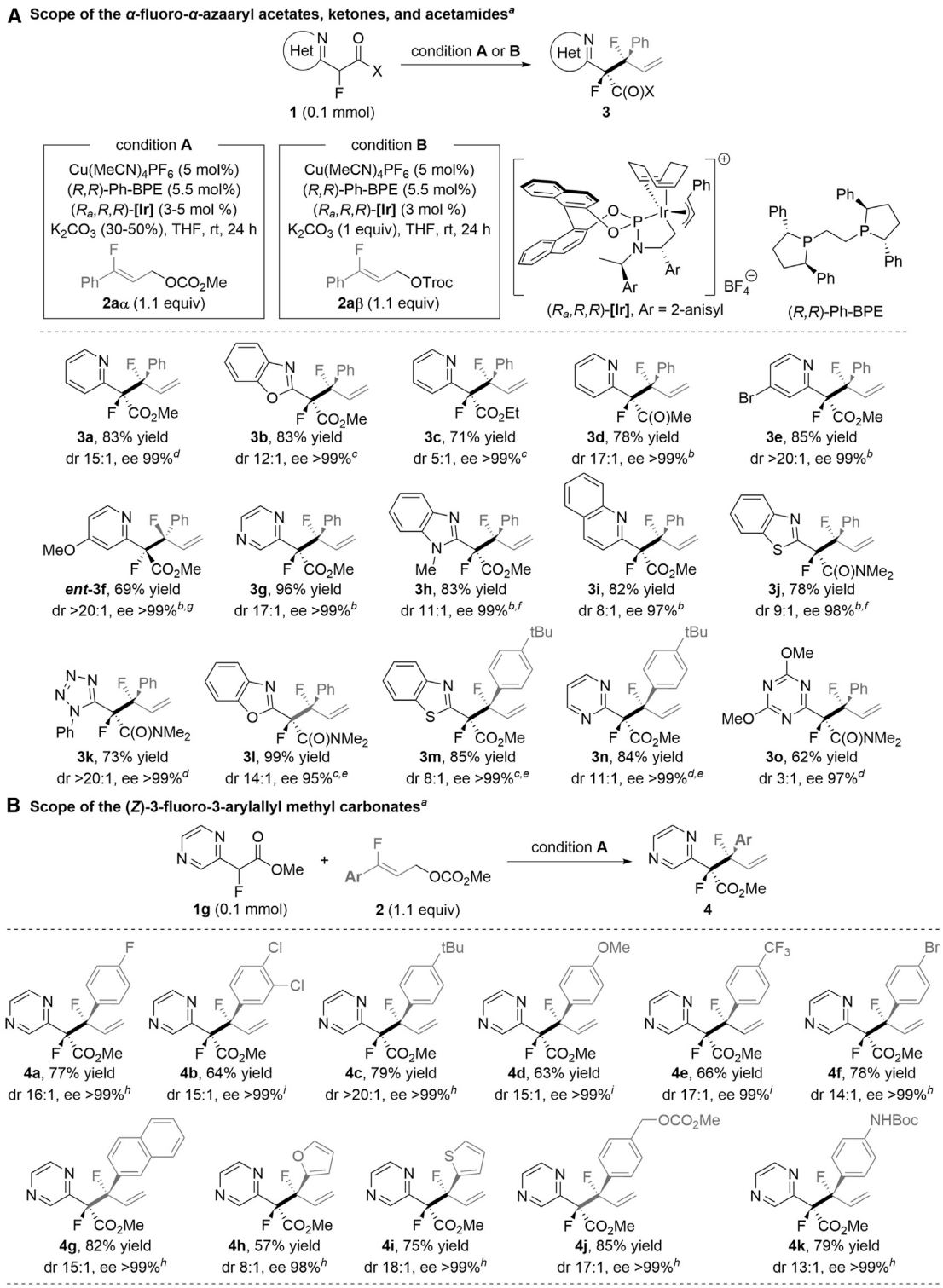

[a]Isolated yield of single diastereomer unless noted otherwise. Diastereomeric ratio (dr) was determined by ^{19}F NMR spectroscopy of the crude reaction mixture. Enantiomeric excess (ee) was determined by chiral HPLC analysis of the isolated major diastereomer. [b]Condition A, 3% [Ir] and 30% K_2CO_3; [c]condition B; [d]condition A, 5% [Ir] and 50% K_2CO_3; [e]combined yield of both diastereomers; [f]48 h instead of 24 h; [g](*S,S*)-Ph-BPE and (S_a,*S,S*)-[Ir] were used; [h]3% [Ir] and 30% K_2CO_3; [i]5% [Ir] and 50% K_2CO_3.

Figure 2. Scope of pronucleophiles and electrophiles that form vicinal difluorides stereoselectively

(A) Scope of the α-fluoro-α-azaaryl acetates, ketones, and acetamides for the catalytic fluoroallylation reaction and (B) scope of the (*Z*)-3-fluoro-3-arylallyl methyl carbonates that undergo the catalytic allylic substitution with methyl 2-pyrazinyl α-fluoroacetate (**1g**).

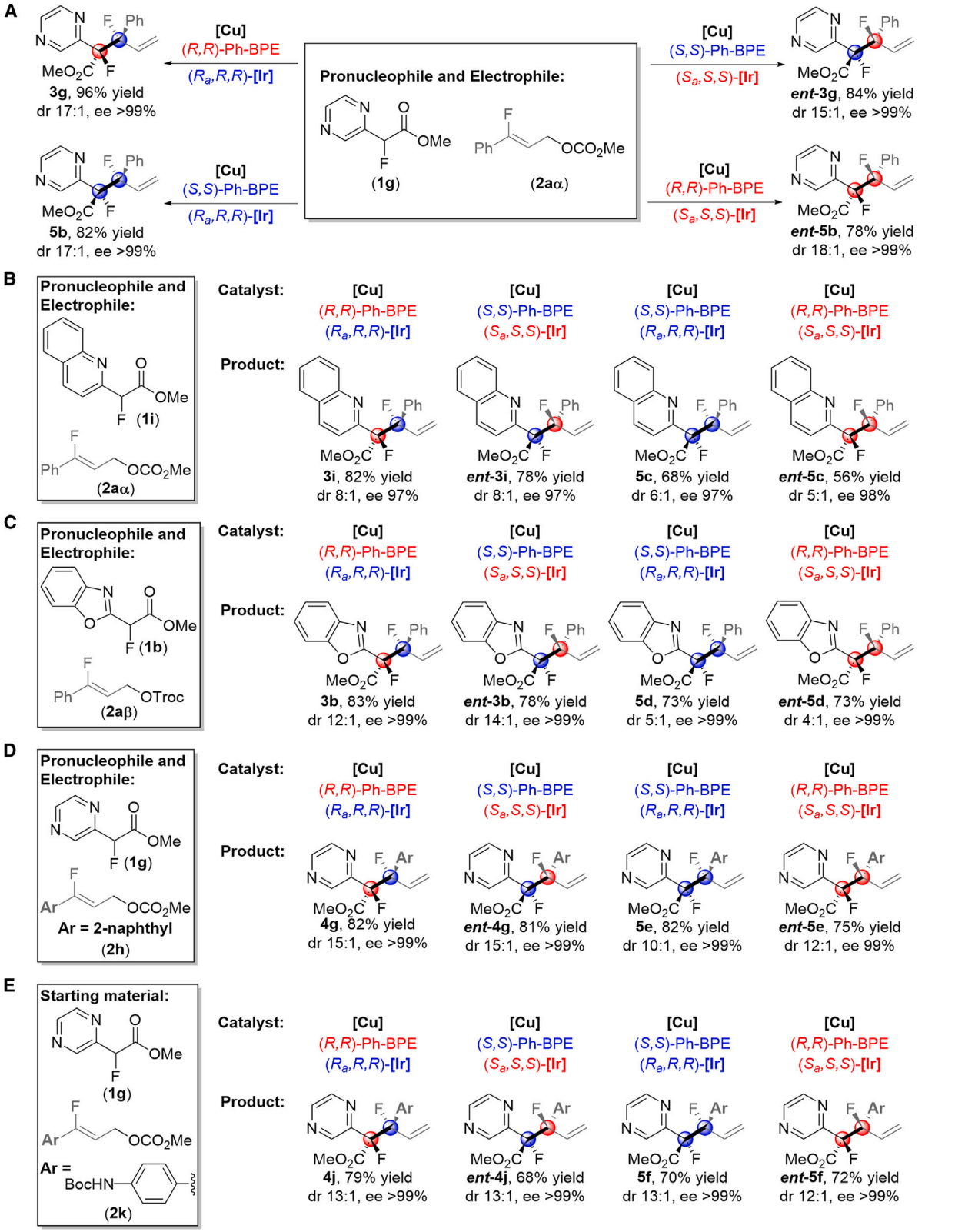

(legend on next page)

Demonstration of stereodivergent synthesis

Results from Figure 3 show that this reaction to form the C–C bond between vicinal fluorides stereoselectively can be used to synthesize each of the four stereoisomers. These reactions were conducted in this stereodivergent fashion to form products containing a six-membered (Figures 3A and 3B) or a five-membered heteroarene (Figure 3C), as well as those containing various unsubstituted or substituted arenes (Figures 3D and 3E). Each stereoisomer of a given vicinal difluoride product in Figure 3 was synthesized in good yield (56%–96%) with synthetically useful to high diastereoselectivity (dr 4:1–18:1) and with excellent enantioselectivity (ee 97%–99%) from the same, optically inactive starting materials by simple permutation of the enantiomers of the Cu and the Ir catalysts. The heteroaryl group on the azaaryl ester unit provides a defined structure to the copper-substrate complex and is the type of subunit in a wide range of small molecules with biological activities.[65–70]

Evidence for a *gauche* relationship between fluorine atoms in the vicinal difluoride products

One could imagine that the large and polar groups on the carbon atoms of the vicinal difluoride would dominate the conformation about the vicinal difluoride unit. However, X-ray crystallographic data of the vicinal difluoride compound **4g**, which was synthesized from the allylic substitution in the presence of catalytic amounts of (*R,R*)-Ph-BPE (**L6**) and (R_a,*R,R*)-**[Ir]**, show that the two C–F bonds in **4g** occupy a *gauche* relationship in the solid-state structure of the compound and that the two aryl groups, which are the two largest substituents, occupy positions *anti* to each other (Figure 4A). While this conformation could be the result of minimizing steric repulsion between these two large groups, the X-ray crystallographic data of compound *ent*-**5d**, which was synthesized from the reaction with (*R,R*)-Ph-BPE and (S_a,*S,S*)-**[Ir]** and is, therefore, the other diastereomeric form of the family of vicinal difluorides, indicate that the two C–F bonds in *ent*-**5d** are also located *gauche* to each other in the solid state (Figure 4B) and that the two aryl groups, therefore, occupy positions *gauche* to each other. In contrast, the two small groups occupy positions *anti* to each other to minimize the gauche interactions between the large groups in all reported crystal structures of the analogous compounds containing one fluorine or no fluorine atoms.[53,54] Thus, the properties and interactions of the organic groups can contribute to the observed conformations, but the two fluorine atoms are shown by experiment to maintain their *gauche* relationship.

Density functional theory (DFT) calculations of the relative free energies of the *anti* and *gauche* conformers of the two pairs of diastereomers **3a**, **5a** and **3b**, **5d** in the solution phase (see the supplemental information for computational details) are consistent with this finding. The computed energies of the *gauche* conformers are lower than those of the other conformations (1.2–1.9 kcal/mol lower in energy than the *anti* conformers) in all cases (Figure 4C). These results indicate that the *gauche* conformation of the two adjacent C–F bonds dictates the most stable structure of these molecules, despite the potential steric repulsion between the heteroarene and the arene attached to the two adjacent carbons or the effect of the polarity of the alkoxycarbonyl unit. The computed energies by DFT calculations of the monofluoro analogs of these molecules containing a fluorine atom alpha to the carbonyl unit are distinct from those of the difluorides (see Figure S4 of the supplemental information). The conformation of the monofluorides containing the hydrogen and fluorine *anti* to each other is computed to be 0.6 to 3.1 kcal/mol more stable, depending on the stereoisomer, than a conformer with hydrogen and fluorine *gauche* to each other. These data imply that the two fluorines in the vicinal difluorides stabilize the gauche conformation in these structures relative to the analogous structures containing one fluorine by no less than 2 kcal/mol.

The ability to synthesize all four stereoisomers of the vicinal difluoride compounds (Figure 3) and the low energy of the conformation with the two C–F bonds *gauche* to each other (Figure 4) demonstrate that one can generate a range of molecular structures containing an acyclic C(sp^3)–C(sp^3) bond from the same reactants by synthesizing the corresponding stereoisomers of a vicinal difluoride. For example, if one considers the structures of diastereomers **3a** and **5a** and seeks a structure in which the pyridyl and the phenyl groups are located *anti* to each other, then one should synthesize diastereomer **3a**; likewise, if one seeks a structure in which the pyridyl and the phenyl groups are located *gauche* to each other, then stereoisomer **5a** should be synthesized. Thus, we have developed a working strategy to control the conformation of acyclic C(sp^3)–C(sp^3) bonds by synthesizing the desired stereoisomer of the vicinal difluoride motif in a modular fashion via C–C bond formation.

Chemical proteomic experiments to assess binding of vicinal difluoride stereoisomers

To assess the effect of our convergent preparation of vicinal difluoride stereoisomers on their interactions with proteins, we synthesized compounds **8a–d**, which constitute a set of four stereoisomers containing photoreactive probes.[71,72] We prepared **8a–d** from the vicinal difluoride compound **4d** and its three stereoisomers *ent*-**4d**, **5g**, and *ent*-**5g**, all of which contain a pyrazine and a methoxy substituent that could assist binding to proteins by hydrogen bonds (see Figure 5A and the supplemental information for details of the synthesis). Thus, compounds **8a–d** possess a small-molecule fragment that would engage in non-covalent interactions with proteins (the vicinal difluoride moiety containing the pyrazine and the 4-methoxyphenyl group shown in the orange box of Figure 5C), a photoreactive diazirine group (blue box of Figure 5C), which forms, by photoirradiation, a carbene intermediate that covalently binds to the protein interacting with the probe, and a terminal alkyne (red box of Figure 5C), which can undergo click reactions for the detection, enrichment, identification, or visualization of the interacting protein.[73] Because the lowest-energy conformers of probes **8a–d** are different, we envisioned that the identity of the proteins to which they bind and

Figure 3. Demonstration of stereodivergent synthesis

(A) Reaction scheme for the stereodivergent synthesis of a set of four stereoisomers: **3g**, **5b**, ***ent*-3g**, and ***ent*-5b**.

(B–E) Additional examples of stereodivergent synthesis.

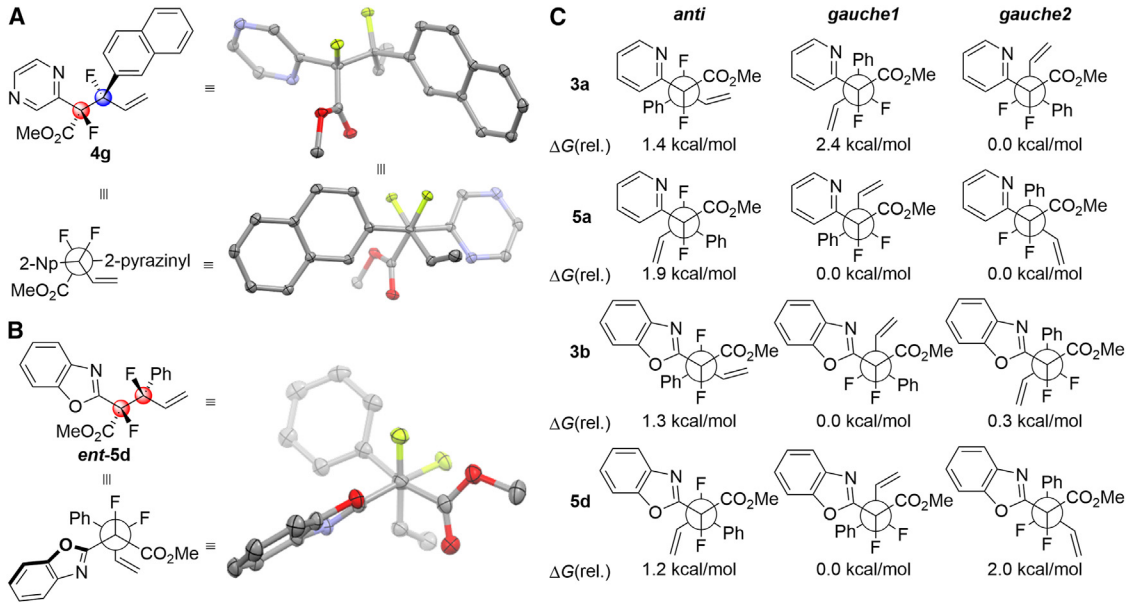

Figure 4. Evidence for the gauche relationship between two fluorine atoms

(A) The *gauche* conformation of the two C(sp^3)–F bonds in vicinal difluoride compound **4g** shown from the side and down the C–C bond, (B) compound *ent*-**5d** shown down the C–C bond determined by single-crystal X-ray diffraction, and (C) calculated relative Gibbs free energies (Δ*G*(rel.)) of the *anti* and *gauche* conformers of vicinal difluoride compounds **3a**, **5a**, **3b**, and **5d**.

the strength of such binding will be different and that such differences would become evident in chemical proteomic experiments.

To assess visually whether the individual stereoisomers of **8a**–**8d** exhibited differences in protein binding, we labeled HEK293T proteomes with each probe, followed by irradiation of the proteome to photocrosslink the probes to their respective protein targets. We then appended an azide-functionalized rhodamine handle by copper-catalyzed azide-alkyne cycloaddition (CuAAC) and visualized the probe-labeled proteins by sodium dodecylsulfate polyacrylamide gel electrophoresis (SDS/PAGE) and in-gel fluorescence (Figure 6A). Consistent with our hypothesis, we observed differential binding of proteins to each stereoisomer, with more pronounced labeling of targets by isomer **8c** than by the other three isomers (Figure 6A).

To identify the proteins specifically labeled by each probe and to identify potential stereospecific ligand-protein binding interactions, we performed chemoproteomic profiling of the interactions of **8a**–**8d** in HEK293T cells (Figures 6B and S3). We treated HEK293T cells with **8a**–**8d** for 30 min. Harvested proteomes were then subjected to CuAAC with an azide-functionalized biotin enrichment handle. Probe-labeled proteins were avidin-enriched, eluted, and analyzed by liquid chromatography-mass spectrometry (LC-MS/MS).

Consistent with the gel-based analysis indicating the highest degree of protein labeling with **8c**, followed by its enantiomer **8b**, and substantially less labeling with their diastereomers **8d** and **8a**, we observed 61 and 34 proteins that were significantly enriched and identified with **8c** and **8b**, respectively. No proteins were significantly enriched over vehicle-treated controls with **8d** and **8a** (Figures 6B and S3). Among proteins that were commonly identified across all four chemoproteomic comparisons with **8a**–**8d**, TXNRD2 was significantly enriched by **8c** with a ratio of enrichment of 6.82 over the control with DMSO vehicle. In contrast, ratios of enrichment with compounds **8a**, **8b**, and **8d** were merely 1.03, 1.06, and 0.99, respectively (Figures 6B and S3). To corroborate these proteomic results, we conducted western blot pull-down. This experiment showed that treatment of HEK293T cells with **8c** but not with **8a**, **8b**, or **8d** led to labeling of TXNRD2 and did not lead to detectable labeling of unrelated targets, such as GAPDH (Figure 6C).

To further assess the role of the vicinal difluoride unit, we conducted parallel experiments with the monofluoro compounds **9a**–**d**. No proteins were significantly enriched by the proteomic protocol with compounds **9a**, **9c**, and **9d**, and only 20 proteins were observed to engage significantly with **9b** (Figure S3; Table S2). TXNRD2 was detected, but it was not significantly enriched by any of the monofluoro compounds. This large difference in binding affinities between the monofluoro compounds and the vicinal difluorides is consistent with the latter compounds adopting defined conformations and is inconsistent with a difference in affinity resulting from changes in non-covalent intermolecular interactions, such as H-bonding, or changes in lipophilicity caused by the additional fluorine atom in **8a**–**d**. The H-bonding to tertiary alkyl fluorides is known to be weak,[74] the difference in hydrophobicity between monofluoro and difluoroalkyl motifs is known to be small,[75] and these differences would be insensitive to stereochemistry. Indeed, the computed values for partition coefficient (logP or ClogP) and topological polar surface area (TPSA) of two sets of four stereoisomers of the mono-fluorinated and difluorinated compounds are indistinguishable (see supplemental information). Thus, all our data demonstrate that the catalytic,

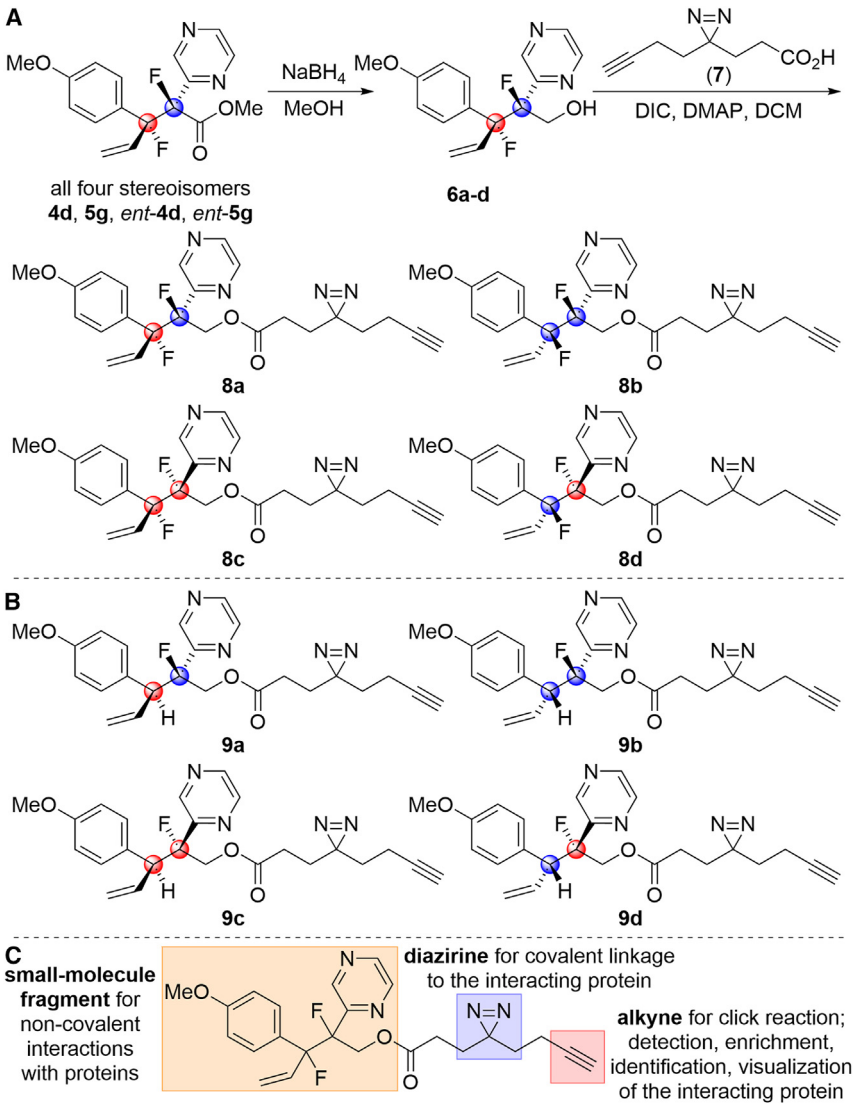

Figure 5. Design and synthesis of probes for chemical proteomics

(A) Synthesis of probes **8a–d** from all four stereoisomers of the vicinal difluoride compound **4d**.

(B) The mono-fluorinated analogs **9a–d** were prepared for control experiments.

(C) The three important components of a probe for fragment-based chemical proteomics.

stereodivergent construction of acyclic vicinal difluoride units can be used to generate unique stereoisomeric chemoproteomic probes that participate in stereospecific ligand-protein interactions.

Conclusion

Together, this work shows that the formation of vicinal fluorides by constructing the core C–C bond with stereoselective catalysts that join two simple racemic or achiral monofluoro components creates the potential to increase protein binding by controlling the population of multiple conformations that are similar in energy in the absence of fluorine. In general, this strategy to form vicinal difluorides by formation of C–C bonds will be valuable for achieving conformational control in molecules containing highly substituted C(sp^3)–C(sp^3) bonds and connects the concept of stereodivergent synthesis to the binding of resulting stereoisomeric products to biological macromolecules. Thus, this synthetic strategy can now be part of the design of molecular structures that alter a wide range of biological functions to improve human health.

EXPERIMENTAL PROCEDURES

General procedure for the stereoselective synthesis of vicinal difluorides

In a nitrogen-filled glovebox, a 4 mL vial equipped with a magnetic stir bar was charged with $[Cu(MeCN)_4]PF_6$ (9.3 mg, 0.025 mmol), (*R,R*)-Ph-BPE (13.9 mg, 0.0275 mmol), and THF (1.5 mL) and stirred at room temperature for 30 min to prepare the stock solution of the copper complex (solution **A**). Another 4 mL vial equipped with a magnetic stir bar was charged with the pronucleophile (0.11 mmol) and solution **A** (0.33 mL), and the resulting solution was stirred at room temperature for 15 min (solution **B**). To a third 4 mL vial equipped with a magnetic stir bar was added sequentially the **[Ir]** catalyst (3.3 mg, 0.0030 mmol, 3 mol % or 5.5 mg, 0.0050 mmol, 5 mol %), K_2CO_3 (4.1 mg, 0.030 mmol, 0.30 equiv or 13.8 mg, 0.100 mmol, 1.000 equiv), the electrophile (0.11 mmol), THF (0.3 mL), and finally solution **B** (0.3 mL). The vial was capped,

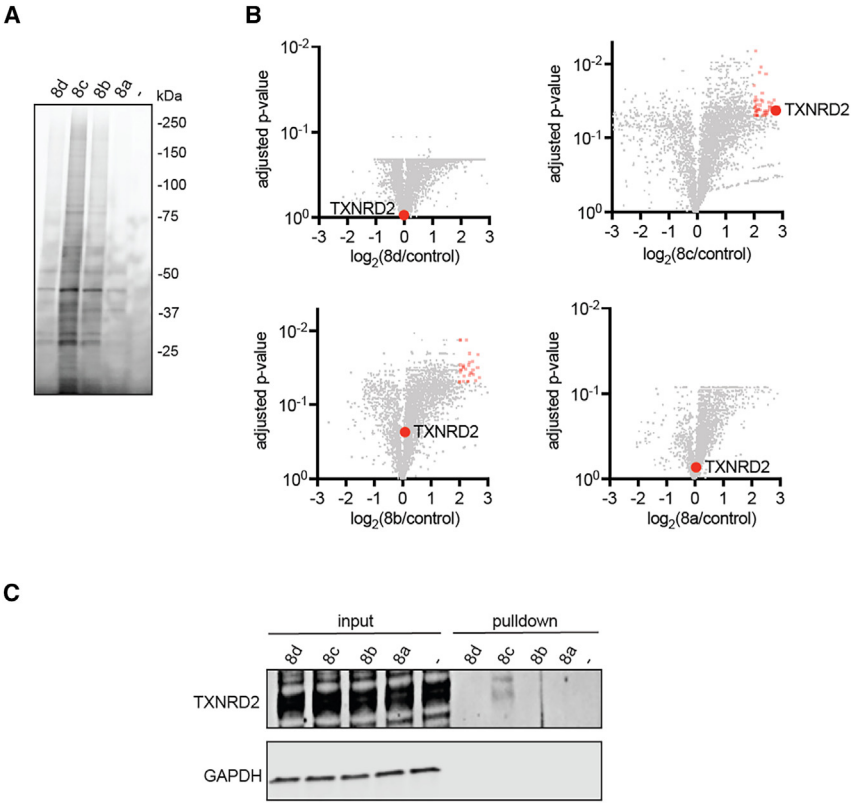

Figure 6. Results from chemoproteomic profiling

(A) Fluorescent detection of ligand-protein binding in HEK293T cells. HEK293T cells were treated with DMSO vehicle or probes **8a–8d** (20 μM) for 30 min, followed by irradiation. The resulting cell lysates were appended to an azide-functionalized rhodamine by CuAAC and visualized by SDS/PAGE and in-gel fluorescence.

(B) Chemoproteomic profiling of proteins that were labeled and enriched by **8a–8d**. HEK293T cells were treated with DMSO vehicle or **8a–8d** (20 μM) for 30 min prior to irradiation. Probe-labeled proteins from resulting cell lysates were subsequently appended to an azide-functionalized biotin handle by CuAAC, avidin-enriched, eluted, and analyzed by LC-MS/MS.

(C) Validation of the interactions of **8a–8d** with TXNRD2 and unrelated protein glyceraldehyde 3-phosphate dehydrogenase (GAPDH) by western blot pull-down. HEK293T cells were treated with DMSO vehicle or **8a–8d** (20 μM) for 2 h, and, after avidin enrichment and elution, proteins were separated by SDS/PAGE. Both the input and pull-down eluate were blotted for TXNRD2 and GAPDH. All experimental data are from $n = 3$ biologically independent replicates/group.

and the reaction mixture was stirred at room temperature in the glovebox for 24 h. The reaction vial was then removed from the glovebox, and hexane (approx. 1.5 mL) was added to the reaction mixture and stirred for 30 min. The mixture was then filtered through a plug (approx. 3 cm) of silica gel, eluted with 1:1 (v/v) hexanes/EtOAc (100% EtOAc was used for highly polar products), and the filtrate was concentrated *in vacuo*. To this crude mixture was added a stock solution of 1,3,5-trimethoxybenzene (TMB) in $CDCl_3$ (0.05 mL, 0.67 M, 0.33 equiv) as the internal standard. This mixture was further diluted with $CDCl_3$ (approx. 0.55 mL) and subjected to analysis by ^1H and ^{19}F NMR to determine the dr of the reaction. Finally, the crude mixture was purified by column chromatography to afford the vicinal difluoride product as either a single diastereomer or a mixture of diastereomers.

RESOURCE AVAILABILITY

Lead contact

Further information and requests for resources should be directed to and will be fulfilled by the lead contact, John F. Hartwig (jhartwig@berkeley.edu).

Materials availability

Unique and stable reagents generated in this study will be made available on request, but we might require a payment and/or a completed materials transfer agreement if there is potential for commercial application. The supplemental experimental procedures, characterizations of compounds, and details of chemoproteomic studies are described in the supplemental information. Crystallographic data are available from the Cambridge Crystallographic Data Center (CCDC) with deposition numbers 2365700 and 2365701.

Data and code availability

All data needed to support the conclusions of this manuscript are included in the main text or the supplemental information.

ACKNOWLEDGMENTS

We acknowledge NSF (CHE-1565886) and NIH/NCI (R35CA263814) for providing funding for this research. We thank Dr. T.J. O'Connor for helpful discussions on the synthesis of fluorinated electrophiles and Dr. Dan He for assistance with protein binding assays. We thank Dr. Hasan Celik and the College of Chemistry NMR facility (CoC-NMR) at UC Berkeley for spectroscopic assistance. Instruments in the CoC-NMR are supported in part by NIH S10OD024998. We thank the QB3/Chemistry Mass Spectrometry Facility for assistance with high-resolution mass spectrometry. We thank Dr. Kathy Durkin and Dr. Dave Small at the Molecular Graphics and Computation Facility (MGCF) at UC Berkeley for assistance with DFT calculations. Computing resources at the MGCF are supported in part by NIH S10OD034382. We thank Dr. Nicholas Settineri, Isaac F. Yu, and the College of Chemistry X-ray Crystallography Facility (CheXray) at UC Berkeley for assistance with crystallography. CheXray is supported in part by NIH S10RR027172.

AUTHOR CONTRIBUTIONS

J.F.H., D.K.N., Y.Q., and X.J. conceived and created an initial design of the project. Y.Q. synthesized compounds, developed reaction conditions, and conducted computational studies. V.C.J.X.T. conducted the chemoproteomic experiments. T.F. and Z.-T.H. assisted in the synthesis of compounds. R.C. assisted in the protein binding assays. T.W.B. developed a method for the synthesis of the photoreactive fragment. Y.Q., V.C.J.X.T., D.K.N., and J.F.H. analyzed the results from experiments and drafted the initial paper. All authors contributed to or approved the final version of the paper.

DECLARATION OF INTERESTS

D.K.N. is a co-founder, shareholder, and scientific advisory board member for Frontier Medicines and Vicinitas Therapeutics. D.K.N. is a member of the board of directors for Vicinitas Therapeutics. D.K.N. is also on the scientific

advisory board for The Mark Foundation for Cancer Research, Photys Therapeutics, Apertor Pharmaceuticals, and Oerth Bio. D.K.N. is also an Investment Advisory Partner for a16z Bio+Health, an advisory board member for Droia Ventures, and an iPartner at The Column Group.

SUPPLEMENTAL INFORMATION

Supplemental information can be found online at https://doi.org/10.1016/j.chempr.2024.08.024.

Received: April 23, 2024
Revised: June 27, 2024
Accepted: August 29, 2024
Published: September 30, 2024

REFERENCES

1. Zheng, Y., Tice, C.M., and Singh, S.B. (2017). Conformational control in structure-based drug design. Bioorg. Med. Chem. Lett. *27*, 2825–2837. https://doi.org/10.1016/j.bmcl.2017.04.079.
2. Hantschel, O. (2015). Unexpected Off-Targets and Paradoxical Pathway Activation by Kinase Inhibitors. ACS Chem. Biol. *10*, 234–245. https://doi.org/10.1021/cb500886n.
3. Anami, Y., Itoh, T., Egawa, D., Yoshimoto, N., and Yamamoto, K. (2014). A Mixed Population of Antagonist and Agonist Binding Conformers in a Single Crystal Explains Partial Agonism against Vitamin D Receptor: Active Vitamin D Analogues with 22R-Alkyl Group. J. Med. Chem. *57*, 4351–4367. https://doi.org/10.1021/jm500392t.
4. Patrick, G.L. (2013). An Introduction to Medicinal Chemistry, Fifth Edition (Oxford University Press).
5. Nadendla, E., Teyssier, C., Delfosse, V., Vivat, V., Krishnasamy, G., Gronemeyer, H., Bourguet, W., and Germain, P. (2015). An Unexpected Mode Of Binding Defines BMS948 as A Full Retinoic Acid Receptor β (RARβ, NR1B2) Selective Agonist. PLoS One *10*, e0123195. https://doi.org/10.1371/journal.pone.0123195.
6. Kazui, Y., Fujii, S., Yamada, A., Ishigami-Yuasa, M., Kagechika, H., and Tanatani, A. (2018). Structure-activity relationship of novel (benzoylaminophenoxy)phenol derivatives as anti-prostate cancer agents. Bioorg. Med. Chem. *26*, 5118–5127. https://doi.org/10.1016/j.bmc.2018.09.008.
7. Kagechika, H., Himi, T., Kawachi, E., and Shudo, K. (1989). Retinobenzoic acids. 4. Conformation of aromatic amides with retinoidal activity. Importance of trans-amide structure for the activity. J. Med. Chem. *32*, 2292–2296. https://doi.org/10.1021/jm00130a011.
8. Robello, M., Barresi, E., Baglini, E., Salerno, S., Taliani, S., and Settimo, F.D. (2021). The Alpha Keto Amide Moiety as a Privileged Motif in Medicinal Chemistry: Current Insights and Emerging Opportunities. J. Med. Chem. *64*, 3508–3545. https://doi.org/10.1021/acs.jmedchem.0c01808.
9. McDowell, R.S., Blackburn, B.K., Gadek, T.R., McGee, L.R., Rawson, T., Reynolds, M.E., Robarge, K.D., Somers, T.C., and Thorsett, E.D. (1994). From Peptide to Non-Peptide. 2. The de Novo Design of Potent, Non-peptidal Inhibitors of Platelet Aggregation Based on a Benzodiazepinedione Scaffold. J. Am. Chem. Soc. *116*, 5077–5083. https://doi.org/10.1021/ja00091a008.
10. Chow, Y.L., Colón, C.J., and Tam, J.N.S. (1968). A(1,3) interaction and conformational energy of axial–axial 1,3-dimethyl interaction. Can. J. Chem. *46*, 2821–2825. https://doi.org/10.1139/v68-467.
11. Lotesta, S.D., Marcus, A.P., Zheng, Y., Leftheris, K., Noto, P.B., Meng, S., Kandpal, G., Chen, G., Zhou, J., McKeever, B., et al. (2016). Identification of spirooxindole and dibenzoxazepine motifs as potent mineralocorticoid receptor antagonists. Bioorg. Med. Chem. *24*, 1384–1391. https://doi.org/10.1016/j.bmc.2016.02.014.
12. Tang, L., Gamal El-Din, T.M., Swanson, T.M., Pryde, D.C., Scheuer, T., Zheng, N., and Catterall, W.A. (2016). Structural basis for inhibition of a voltage-gated Ca2+ channel by Ca2+ antagonist drugs. Nature *537*, 117–121. https://doi.org/10.1038/nature19102.
13. Wang, Y., Kirschner, A., Fabian, A.-K., Gopalakrishnan, R., Kress, C., Hoogeland, B., Koch, U., Kozany, C., Bracher, A., and Hausch, F. (2013). Increasing the Efficiency of Ligands for FK506-Binding Protein 51 by Conformational Control. J. Med. Chem. *56*, 3922–3935. https://doi.org/10.1021/jm400087k.
14. Xu, Z., Tice, C.M., Zhao, W., Cacatian, S., Ye, Y.-J., Singh, S.B., Lindblom, P., McKeever, B.M., Krosky, P.M., Kruk, B.A., et al. (2011). Structure-Based Design and Synthesis of 1,3-Oxazinan-2-one Inhibitors of 11β-Hydroxysteroid Dehydrogenase Type 1. J. Med. Chem. *54*, 6050–6062. https://doi.org/10.1021/jm2005354.
15. Carder, H.M., Wang, Y., and Wendlandt, A.E. (2022). Selective Axial-to-Equatorial Epimerization of Carbohydrates. J. Am. Chem. Soc. *144*, 11870–11877. https://doi.org/10.1021/jacs.2c04743.
16. Solel, E., Ruth, M., and Schreiner, P.R. (2021). London Dispersion Helps Refine Steric A-Values: The Halogens. J. Org. Chem. *86*, 7701–7713. https://doi.org/10.1021/acs.joc.1c00767.
17. Jensen, F.R., Bushweller, C.H., and Beck, B.H. (1969). Conformational preferences in monosubstituted cyclohexanes determined by nuclear magnetic resonance spectroscopy. J. Am. Chem. Soc. *91*, 344–351. https://doi.org/10.1021/ja01030a023.
18. Basso, E.A., Kaiser, C., Rittner, R., and Lambert, J.B. (1993). Axial/equatorial proportions for 2-substituted cyclohexanones. J. Org. Chem. *58*, 7865–7869. https://doi.org/10.1021/jo00079a035.
19. Pennington, L.D., and Moustakas, D.T. (2017). The Necessary Nitrogen Atom: A Versatile High-Impact Design Element for Multiparameter Optimization. J. Med. Chem. *60*, 3552–3579. https://doi.org/10.1021/acs.jmedchem.6b01807.
20. Lynch, S.M., DeVicente, J., Hermann, J.C., Jaime-Figueroa, S., Jin, S., Kuglstatter, A., Li, H., Lovey, A., Menke, J., Niu, L., et al. (2013). Strategic use of conformational bias and structure based design to identify potent JAK3 inhibitors with improved selectivity against the JAK family and the kinome. Bioorg. Med. Chem. Lett. *23*, 2793–2800. https://doi.org/10.1016/j.bmcl.2013.02.012.
21. Clayden, J., Moran, W.J., Edwards, P.J., and LaPlante, S.R. (2009). The Challenge of Atropisomerism in Drug Discovery. Angew. Chem. Int. Ed. Engl. *48*, 6398–6401. https://doi.org/10.1002/anie.200901719.
22. Glunz, P.W. (2018). Recent encounters with atropisomerism in drug discovery. Bioorg. Med. Chem. Lett. *28*, 53–60. https://doi.org/10.1016/j.bmcl.2017.11.050.
23. LaPlante, S.R., Edwards, P.J., Fader, L.D., Jakalian, A., and Hucke, O. (2011). Revealing Atropisomer Axial Chirality in Drug Discovery. ChemMedChem *6*, 505–513. https://doi.org/10.1002/cmdc.201000485.
24. Mo, Y. (2011). Rotational barriers in alkanes. WIREs Comput. Mol. Sci. *1*, 164–171. https://doi.org/10.1002/wcms.22.
25. Tsuzuki, S., Uchimaru, T., and Tanabe, K. (1995). Conformational analysis of n-alkanes using density functional theory. Comparison with ab initio calculations. Chem. Phys. Lett. *246*, 9–12. https://doi.org/10.1016/0009-2614(95)01081-J.
26. Thomas, L.L., Christakis, T.J., and Jorgensen, W.L. (2006). Conformation of Alkanes in the Gas Phase and Pure Liquids. J. Phys. Chem. B *110*, 21198–21204. https://doi.org/10.1021/jp064811m.
27. Veber, D.F., Johnson, S.R., Cheng, H.-Y., Smith, B.R., Ward, K.W., and Kopple, K.D. (2002). Molecular Properties That Influence the Oral Bioavailability of Drug Candidates. J. Med. Chem. *45*, 2615–2623. https://doi.org/10.1021/jm020017n.
28. Congreve, M., Carr, R., Murray, C., and Jhoti, H. (2003). A 'Rule of Three' for fragment-based lead discovery? Drug Discov. Today *8*, 876–877. https://doi.org/10.1016/S1359-6446(03)02831-9.
29. O'Hagan, D., Rzepa, H.S., Schüler, M., and Slawin, A.M.Z. (2006). The vicinal difluoro motif: The synthesis and conformation of erythro- and threo-diastereoisomers of 1,2-difluorodiphenylethanes, 2,3-difluorosuccinic acids

and their derivatives. Beilstein J. Org. Chem. *2*, 19. https://doi.org/10.1186/1860-5397-2-19.

30. O'Hagan, D. (2008). Understanding organofluorine chemistry. An introduction to the C–F bond. Chem. Soc. Rev. *37*, 308–319. https://doi.org/10.1039/B711844A.
31. Luo, Y.-R. (2003). Handbook of Bond Dissociation Energies in Organic Compounds (CRC Press).
32. Schüler, M., O'Hagan, D., and Slawin, A.M.Z. (2005). The vicinal F–C–C–F moiety as a tool for influencing peptide conformation. Chem. Commun. (Camb), 4324–4326. https://doi.org/10.1039/B506010A.
33. Gillis, E.P., Eastman, K.J., Hill, M.D., Donnelly, D.J., and Meanwell, N.A. (2015). Applications of Fluorine in Medicinal Chemistry. J. Med. Chem. *58*, 8315–8359. https://doi.org/10.1021/acs.jmedchem.5b00258.
34. Thiehoff, C., Rey, Y.P., and Gilmour, R. (2017). The Fluorine Gauche Effect: A Brief History. Isr. J. Chem. *57*, 92–100. https://doi.org/10.1002/ijch.201600038.
35. Buissonneaud, D.Y., van Mourik, T., and O'Hagan, D. (2010). A DFT study on the origin of the fluorine gauche effect in substituted fluoroethanes. Tetrahedron *66*, 2196–2202. https://doi.org/10.1016/j.tet.2010.01.049.
36. Goodman, L., Gu, H., and Pophristic, V. (2005). Gauche Effect in 1,2-Difluoroethane. Hyperconjugation, Bent Bonds, Steric Repulsion. J. Phys. Chem. A *109*, 1223–1229. https://doi.org/10.1021/jp046290d.
37. Trindle, C., Crum, P., and Douglass, K. (2003). G2(MP2) Characterization of Conformational Preferences in 2-Substituted Ethanols (XCH2CH2OH) and Related Systems. J. Phys. Chem. A *107*, 6236–6242. https://doi.org/10.1021/jp034598j.
38. Yamamoto, I., Jordan, M.J.T., Gavande, N., Doddareddy, M.R., Chebib, M., and Hunter, L. (2012). The enantiomers of syn-2,3-difluoro-4-aminobutyric acid elicit opposite responses at the GABAC receptor. Chem. Commun. (Camb) *48*, 829–831. https://doi.org/10.1039/C1CC15816C.
39. Hamatani, T., Matsubara, S., Matsuda, H., and Schlosser, M. (1988). A stereocontrolled access to vicinal difluoroalkanes. Tetrahedron *44*, 2875–2881. https://doi.org/10.1016/S0040-4020(88)90023-3.
40. Hudlický, M. (1983). Hydrogenolysis of carbon-fluorine bonds in catalytic hydrogenation. II. J. Fluor. Chem. *23*, 241–259. https://doi.org/10.1016/S0022-1139(00)85130-1.
41. Burmakov, A.I., Motnyak, L.A., Kunshenko, B.V., Alexeeva, L.A., and Yagupolskii, L.M. (1981). Treatment of dimethyl (+)-L-tartrate with sulfur tetrafluoride. J. Fluor. Chem. *19*, 151–161. https://doi.org/10.1016/S0022-1139(00)81331-7.
42. Banik, S.M., Medley, J.W., and Jacobsen, E.N. (2016). Catalytic, Diastereoselective 1,2-Difluorination of Alkenes. J. Am. Chem. Soc. *138*, 5000–5003. https://doi.org/10.1021/jacs.6b02391.
43. Molnár, I.G., and Gilmour, R. (2016). Catalytic Difluorination of Olefins. J. Am. Chem. Soc. *138*, 5004–5007. https://doi.org/10.1021/jacs.6b01183.
44. Hara, S., Nakahigashi, J., Ishi-i, K., Sawaguchi, M., Sakai, H., Fukuhara, T., and Yoneda, N. (1998). Difluorination of Alkenes with Iodotoluene Difluoride. Synlett *1998*, 495–496. https://doi.org/10.1055/s-1998-1714.
45. Olah, G.A., Welch, J.T., Vankar, Y.D., Nojima, M., Kerekes, I., and Olah, J.A. (1979). Synthetic methods and reactions. 63. Pyridinium poly(hydrogen fluoride) (30% pyridine-70% hydrogen fluoride): a convenient reagent for organic fluorination reactions. J. Org. Chem. *44*, 3872–3881. https://doi.org/10.1021/jo01336a027.
46. Merritt, R.F., and Stevens, T.E. (1966). Direct Fluorination of Steroidal Olefins to cis-Vicinal Difluorides. J. Am. Chem. Soc. *88*, 1822–1823. https://doi.org/10.1021/ja00960a047.
47. Tius, M.A. (1995). Xenon difluoride in synthesis. Tetrahedron *51*, 6605–6634. https://doi.org/10.1016/0040-4020(95)00362-C.
48. Doobary, S., and Lennox, A.J.J. (2020). Alkene Vicinal Difluorination: From Fluorine Gas to More Favoured Conditions. Synlett *31*, 1333–1342. https://doi.org/10.1055/s-0040-1707143.
49. Hunter, L., Jolliffe, K.A., Jordan, M.J.T., Jensen, P., and Macquart, R.B. (2011). Synthesis and Conformational Analysis of α,β-Difluoro-γ-amino Acid Derivatives. Chemistry *17*, 2340–2343. https://doi.org/10.1002/chem.201003320.
50. Haj, M.K., Banik, S.M., and Jacobsen, E.N. (2019). Catalytic, Enantioselective 1,2-Difluorination of Cinnamamides. Org. Lett. *21*, 4919–4923. https://doi.org/10.1021/acs.orglett.9b00938.
51. Scheidt, F., Schäfer, M., Sarie, J.C., Daniliuc, C.G., Molloy, J.J., and Gilmour, R. (2018). Enantioselective, Catalytic Vicinal Difluorination of Alkenes. Angew. Chem. Int. Ed. Engl. *57*, 16431–16435. https://doi.org/10.1002/anie.201810328.
52. Meyer, S., Häfliger, J., Schäfer, M., Molloy, J.J., Daniliuc, C.G., and Gilmour, R. (2021). A Chiral Pentafluorinated Isopropyl Group via Iodine(I)/(III) Catalysis. Angew. Chem. Int. Ed. Engl. *60*, 6430–6434. https://doi.org/10.1002/anie.202015946.
53. Jiang, X., Boehm, P., and Hartwig, J.F. (2018). Stereodivergent Allylation of Azaaryl Acetamides and Acetates by Synergistic Iridium and Copper Catalysis. J. Am. Chem. Soc. *140*, 1239–1242. https://doi.org/10.1021/jacs.7b12824.
54. He, Z.-T., Jiang, X., and Hartwig, J.F. (2019). Stereodivergent Construction of Tertiary Fluorides in Vicinal Stereogenic Pairs by Allylic Substitution with Iridium and Copper Catalysts. J. Am. Chem. Soc. *141*, 13066–13073. https://doi.org/10.1021/jacs.9b04440.
55. Butcher, T.W., and Hartwig, J.F. (2018). Enantioselective Synthesis of Tertiary Allylic Fluorides by Iridium-Catalyzed Allylic Fluoroalkylation. Angew. Chem. Int. Ed. Engl. *57*, 13125–13129. https://doi.org/10.1002/anie.201807474.
56. Huo, X., He, R., Zhang, X., and Zhang, W. (2016). An Ir/Zn Dual Catalysis for Enantio- and Diastereodivergent α-Allylation of α-Hydroxyketones. J. Am. Chem. Soc. *138*, 11093–11096. https://doi.org/10.1021/jacs.6b06156.
57. Huo, X., Zhang, J., Fu, J., He, R., and Zhang, W. (2018). Ir/Cu Dual Catalysis: Enantio- and Diastereodivergent Access to α,α-Disubstituted α-Amino Acids Bearing Vicinal Stereocenters. J. Am. Chem. Soc. *140*, 2080–2084. https://doi.org/10.1021/jacs.8b00187.
58. Zhang, Z., Puente, Á., Wang, F., Rahm, M., Mei, Y., Mayr, H., and Prakash, G.K.S. (2016). The Nucleophilicity of Persistent α-Monofluoromethide Anions. Angew. Chem. Int. Ed. Engl. *55*, 12845–12849. https://doi.org/10.1002/anie.201605616.
59. Zhang, Z., Puente, Á., Wang, F., Rahm, M., Mei, Y., Mayr, H., and Prakash, G.K.S. (2016). Corrigendum: The Nucleophilicity of Persistent α-Monofluoromethide Anions. Angew. Chem. Int. Ed. Engl. *55*, 14494. https://doi.org/10.1002/anie.201609842.
60. Chambers, R.D. (2004). Fluorine in Organic Chemistry (Blackwell Publishing Ltd./CRC Press).
61. Hine, J., Thomas, C.H., and Ehrenson, S.J. (1955). The Effect of Halogen Atoms on the Reactivity of Other Halogen Atoms in the Same Molecule. V. The SN2 Reactivity of Methylene Halides1. J. Am. Chem. Soc. *77*, 3886–3889. https://doi.org/10.1021/ja01619a061.
62. Martinez, H., Rebeyrol, A., Nelms, T.B., and Dolbier, W.R. (2012). Impact of fluorine substituents on the rates of nucleophilic aliphatic substitution and β-elimination. J. Fluor. Chem. *135*, 167–175. https://doi.org/10.1016/j.jfluchem.2011.10.008.
63. Ni, C., and Hu, J. (2016). The unique fluorine effects in organic reactions: recent facts and insights into fluoroalkylations. Chem. Soc. Rev. *45*, 5441–5454. https://doi.org/10.1039/C6CS00351F.
64. Krautwald, S., Sarlah, D., Schafroth, M.A., and Carreira, E.M. (2013). Enantio- and Diastereodivergent Dual Catalysis: alpha-Allylation of Branched Aldehydes. Science *340*, 1065–1068. https://doi.org/10.1126/science.1237068.
65. Keri, R.S., Patil, M.R., Patil, S.A., and Budagumpi, S. (2015). A comprehensive review in current developments of benzothiazole-based molecules in

medicinal chemistry. Eur. J. Med. Chem. *89*, 207–251. https://doi.org/10.1016/j.ejmech.2014.10.059.

66. Keri, R.S., Hiremathad, A., Budagumpi, S., and Nagaraja, B.M. (2015). Comprehensive Review in Current Developments of Benzimidazole-Based Medicinal Chemistry. Chem. Biol. Drug Des. *86*, 19–65. https://doi.org/10.1111/cbdd.12462.
67. Selvam, T.P., James, C.R., Dniandev, P.V., and Valzita, S.K. (2015). A mini review of pyrimidine and fused pyrimidine marketed drugs. Res. Pharm. *2*.
68. Demmer, C.S., and Bunch, L. (2015). Benzoxazoles and oxazolopyridines in medicinal chemistry studies. Eur. J. Med. Chem. *97*, 778–785. https://doi.org/10.1016/j.ejmech.2014.11.064.
69. Juhás, M., and Zitko, J. (2020). Molecular Interactions of Pyrazine-Based Compounds to Proteins. J. Med. Chem. *63*, 8901–8916. https://doi.org/10.1021/acs.jmedchem.9b02021.
70. Altaf, A.A., Shahzad, A., Gul, Z., Rasool, N., Badshah, A., Lal, B., and Khan, E. (2015). A review on the medicinal importance of pyridine derivatives. J. Drug Med Chem. *1*, 1–11.
71. Parker, C.G., Galmozzi, A., Wang, Y., Correia, B.E., Sasaki, K., Joslyn, C.M., Kim, A.S., Cavallaro, C.L., Lawrence, R.M., Johnson, S.R., et al. (2017). Ligand and Target Discovery by Fragment-Based Screening in Human Cells. Cell *168*, 527–541.e29. https://doi.org/10.1016/j.cell.2016.12.029.
72. Wang, Y., Dix, M.M., Bianco, G., Remsberg, J.R., Lee, H.-Y., Kalocsay, M., Gygi, S.P., Forli, S., Vite, G., Lawrence, R.M., et al. (2019). Expedited mapping of the ligandable proteome using fully functionalized enantiomeric probe pairs. Nat. Chem. *11*, 1113–1123. https://doi.org/10.1038/s41557-019-0351-5.
73. Forrest, I., and Parker, C.G. (2023). Proteome-Wide Fragment-Based Ligand and Target Discovery. Isr. J. Chem. *63*, e202200098. https://doi.org/10.1002/ijch.202200098.
74. Dunitz, J.D., and Taylor, R. (1997). Organic Fluorine Hardly Ever Accepts Hydrogen Bonds. Chemistry A European J. *3*, 89–98. https://doi.org/10.1002/chem.19970030115.
75. Müller, K. (2019). 2 - Fluorination patterns in small alkyl groups: their impact on properties relevant to drug discovery. In Fluorine in Life Sciences: Pharmaceuticals, Medicinal Diagnostics, and Agrochemicals, G. Haufe and F.R. Leroux, eds. (Academic Press), pp. 91–139. https://doi.org/10.1016/B978-0-12-812733-9.00002-7.